coatings

MDPI

Article

Atmospheric Plasma and UV Polymerisation for Developing Sustainable Anti-Adhesive Polyethylene Terephthalate (PET) Surfaces

Tugce Caykara [1,2], Sara Fernandes [1], Adelaide Braga [2], Joana Rodrigues [2], Ligia Raquel Rodrigues [2] and Carla Joana Silva [1,3,*]

[1] CeNTI—Centre for Nanotechnology and Smart Materials, 4760-034 Vila Nova de Famalicão, Portugal
[2] CEB—Centre of Biological Engineering, School of Chemical and Biological Engineering, Universidade do Minho, 4710-057 Braga, Portugal
[3] CITEVE—Portuguese Technological Centre for the Textile and Clothing Industries, Department of Chemical and Biotechnology, 4760-034 Vila Nova de Famalicão, Portugal
* Correspondence: csilva@centi.pt; Tel.:+351-966-896-446

Abstract: Enhancing the hydrophilicity of polymeric materials is an important step for achieving anti-adhesiveness. Thus, in this study, atmospheric plasma as a pre-treatment was combined with a UV grafting process to obtain a durable surface modification on polyethylene terephthalate (PET). The most promising conditions for the atmospheric plasma process were found to be 15 kW power and 4 m/min speed, leading to a contact angle reduction from 70 ± 6° to approximately 30°. However, it was observed that these values increased over time due to the ageing and washing of the PET surface, ultimately causing it to recover its initial contact angle. Therefore, the plasma-pre-treated PET samples were further modified through a UV grafting process using sodium acrylate (NaAc) and 3-sulfopropyl acrylate potassium salts (KAc). The grafted acrylate PET samples exhibited contact angles of 8 ± 3° and 28 ± 13° for NaAc and KAc, respectively, while showing durability in ageing and washing tests. The dry film thicknesses for both samples were found to be 28 ± 2 µm. Finally, the anti-adhesive properties of the NaAc- and KAc-treated surfaces were evaluated using an *Escherichia coli* expressing YadA, an adhesive protein from *Yersinia*. The modified PET surfaces were highly effective in reducing bacterial adhesion by more than 90%.

Keywords: grafting; hydrophilicity; surface modification; wettability; plasma; UV polymerisation

Citation: Caykara, T.; Fernandes, S.; Braga, A.; Rodrigues, J.; Rodrigues, L.R.; Silva, C.J. Atmospheric Plasma and UV Polymerisation for Developing Sustainable Anti-Adhesive Polyethylene Terephthalate (PET) Surfaces. *Coatings* **2023**, *13*, 715. https://doi.org/10.3390/coatings13040715

Academic Editor: Kui Cheng

Received: 20 February 2023
Revised: 27 March 2023
Accepted: 27 March 2023
Published: 31 March 2023

1. Introduction

The number of patients with acquired infections increases every year. The European Centre for Disease Prevention and Control estimated that 8.9 million healthcare-associated infections occur each year in European hospitals and long-term facilities. Additionally, approximately 30% of the bacteria responsible for those infections were found to be resistant to antibiotics [1]. More than ever, it is extremely important to reduce the spread of infections. A potential way to reduce the spread of infections and antibiotic resistance is using anti-adhesive materials that can, in turn, reduce the microbial load on surfaces. A popular approach to obtain such anti-adhesive surfaces is to use hydrophilic surfaces [2] since it has been shown that hydrophilic surfaces can prevent bacterial adhesion by forming a hydration layer [3]. One attractive method for obtaining such surfaces is a plasma treatment. A plasma surface treatment, in particular, cold atmospheric plasma, can be applied to many different materials (metal, wood, paper, glass, polymers, ceramics and nonwoven textiles, among others), and the medical sector is one of its main application fields [4]. Plasma systems are well known, and they can be used for a variety of treatments, such as surface cleaning, etching, functionalisation, activation and polymerisation, since they change the chemical and physical properties of the surface [5,6]. The gas type used in a plasma

system can determine the hydrophilicity and hydrophobicity of the treated surface [2], and hydrophilic surfaces can be obtained by using gases such as air, oxygen, nitrogen, helium and argon [5,7]. The use of atmospheric air as a reactive gas can be a viable option for plasma treatment as it is a natural, ecological, inexpensive and abundant gas mixture [8]. Additionally, since it is a dry surface treatment, using plasma eliminates the need to use harmful chemicals and, consequently, their effluents, leading to more sustainable processes [5]. Furthermore, the use of atmospheric plasma can eliminate the drawbacks of low-pressure plasma systems such as expensive vacuum systems, high maintenance costs and being limited to batch processes and smaller area treatments. Although atmospheric plasma offers these advantages, it has been seldom studied compared to low-pressure plasma [8].

Moreover, UV-induced photopolymerisation is also an attractive technology for both industry and laboratory research as it is characterised as having a low environmental impact and is a versatile technique with a high efficiency. In most cases, a photoinitiator is needed to create the necessary radicals for the initiation of the polymerisation reaction. However, there are drawbacks with the use of photoinitiators, such as storage problems, unwanted odour and colour on final products, migration of the remaining photoinitator molecules, health concerns and costs [9]. Thus, UV can be combined with plasma to generate radicals such as peroxyl or hydroxyl on surfaces [6], increasing the efficiency of the polymerisation reaction and removing the unnecessary use of photoinitiators [6,8,10,11].

In this study, we used polyethylene terephthalate (PET) as a base substrate since it is one of the most popular polymers used in the medical context due to its hardness, stiffness and biocompatibility, as well as its biological, chemical and mechanical stability [2]. However, PET surfaces need to be modified to prevent/reduce bacterial adhesion. Charged polymer networks exhibit a high uptake of water [12], and sodium acrylate (NaAc) and 3-sulfopropyl acrylate potassium salt (KAc) are both used in the preparation of the charged polymers commonly used in hydrogel studies [12,13]. Furthermore, poly(sodium acrylate) is known to be a superabsorbent [14] material and is a good candidate for improving surface hydrophilicity. Thus, a combined process of plasma and UV photopolymerisation for PET modification was employed in this study in order to render the PET surface hydrophilic. An initial statistical study for the determination of the optimal experimental parameters of the plasma treatment (speed and power) using air as a reactive gas was performed. After that, the atmospheric-plasma-treated samples were further subjected to UV polymerisation with NaAc and KAc. Finally, the bacterial anti-adhesive properties of the PET-treated surfaces were assessed.

2. Materials and Methods

2.1. Materials

PET film (Mylar® A with a thickness of 36 μm) was acquired from Isovolta Group, Wiener Neudorf, Austria. Sodium acrylate (97%) and diodomethane (99%) were purchased from Sigma-Aldrich, St. Louis, MO, USA, and 3-sulfopropyl acrylate potassium salt (>98%) was purchased from TCI Chemicals, Tokyo, Japan.

2.2. Pre-Treatment with Atmospheric Plasma

The PET substrates were subjected to a conventional corona treatment using dielectric barrier discharge (DBD) atmospheric pressure plasma equipment (Sigma Technologies International, Tuscon AZ, USA—atmospheric plasma treatment system) at room temperature and with a relative humidity of approximately 45%–55%. This plasma treatment system was designed to handle substrates up to 2 m wide, and the rolls, which were protected with insulating silicon sleeves, had diameters of 30 cm. It was a single-sided treatment, with a maximum web speed of 50 m/min and two metal electrodes (2 m × 3 cm) powered by a mid-frequency generator with a 15 kW power supply. The PET film samples were treated at a power supply that varied from 15 kW (100% of maximum power) to 7.5 kW (50% of

maximum power) and a conveyor speed that ranged from 4 m/min (1.1 Hz) to 12 m/min (3.3 Hz).

2.3. Experimental Design and Optimisation by Response Surface Methodology (RSM)

In the first step, a 2^2 full factorial design (experimental design in which data is collected for all possible combinations of the two factors of interest at two discrete possible levels) was utilised to evaluate the effect of the treatment power and speed on the PET surface modification. The initial water contact angle (WCA), WCA after 2 weeks of ageing and percentage of oxygen increase were used as the response variables. The selected variables and their levels are listed in Table 1. State-Ease® 'Design Expert' (version 12) software was used for the regression and graphical analyses of the data obtained. The statistical significance of the regression coefficients was determined by Student's *t*-test, the second-order model equation was determined by Fischer's test and the proportion of variance was explained by the multiple coefficients of determination, R^2. The optimum range of the variables was obtained by the graphical analysis using the 'Design expert' program.

Table 1. Coded and actual levels for the design of the experiment's variables.

Independent Variables	Factor	Range and Levels		
		−1	**0**	**+1**
Speed (m/min)	A	4	8	12
Power (kW)	B	7.5	11.25	15

2.4. UV Polymerisation of PET with Acrylates

One-hundred g/L of sodium acrylate and 200 g/L of 3-sulfopropyl acrylate potassium salt solutions were prepared with MiliQ water (Merck S.A., Lisbon, Portugal) and purged with nitrogen for 1 h. Meanwhile, the plasma pre-treated PET samples were placed in a Petri dish in a nitrogen atmosphere for 30 min before the addition of the acrylates solution. After the addition of the acrylates solution, they were left in the nitrogen atmosphere for 30 min before starting the UV polymerisation. For the UV polymerisation, an OmniCure S2000 Lumen Dynamics (Mississauga (ON), Canada) equipped with a 200 W mercury vapor short-arc lamp (with an emission spectrum of between 300 nm and 450 nm) was used for 35 min. The grafted samples were rinsed and immersed in distilled water for one day to release any adsorbed acrylates from the surface. Finally, the samples were dried under vacuum conditions for 4 h before any characterisation of the modified surfaces was performed.

2.5. Water Contact Angle (WCA)

The hydrophilicity of the modified surfaces was evaluated by static WCA measurements using the Optical Tensiometer Attension Model Theta Basic by Biolin Scientific, (Gothenburg, Sweden) at room temperature. MiliQ water with a droplet size of 3 µL was used. The measurements were repeated at least 3 times for each sample at different locations. Furthermore, contact angle values after 5 cycles of washing (one cycle of washing consisted of immersing the sample in distilled water at 40 °C with 100 rpm agitation for 30 min) and after 2 and 3 weeks of storage were measured to evaluate the stability and durability of the surface treatment. Contact angle measurements were also performed with diiodomethane in order to allow the calculation of polar and dispersed components of surface energy by the Owens, Wendt, Rabel and Kaelble Model (OWRK) equation [15].

2.6. XPS Analysis

X-ray photoelectron spectroscopy (XPS) analysis (E557-X-ray Photoelectron Spectroscope; Serial Nr. C332844/01; Model Axis Supra; Manufacturer Kratos, Manchester, UK) was used to evaluate the chemical composition of the samples. Monochromatic X-ray source Al Kα (1486.6 eV) was used for all samples and experiments with a take-off angle of

90°. The residual vacuum in the X-ray analysis chamber was maintained at approximately 5.6×10^{-9} Torr. The measurements were completed in a Constant Analyser Energy mode (CAE) with a 10 mA emission current and 160 eV pass energy for the survey spectra and a 15 mA emission current and 40 eV pass energy for the high resolution spectra. Charge referencing was completed by setting the lower binding energy C 1s photo peak at a 285.0 eV C 1s hydrocarbon peak.

2.7. UV-VIS Spectrophotometer

A UV-VIS spectrophotometer (Perkin Elmer Lambda 35, MA, USA) was used for the determination of the film thicknesses of the treated materials. The spectra in transmittance were collected in the wavelength range of 250–1100 nm with three repetitions. The Swanepoel method was used for the calculation of the film thicknesses [16].

2.8. AFM Analysis

A Keysight Technologies 5500 Atomic Force Microscope (Santa Rosa, CA, USA) was used to perform the AFM measurements. The measurements were performed in air in tapping mode (Mac Mode) at room temperature. Silicone material cantilevers with a spring constant of 13–77 N/m and radius < 10 nm were used. The images were analysed using Keysight PicoView 1.20.3 and Gwyddion 2.57 software. All images were taken at a 3 µm × 3 µm surface area.

2.9. Anti-Adhesive Performance

Bacterial adhesion tests were performed according to the methodology previously described [15]. Briefly, the samples were cut to a size of 1 cm × 1.5 cm and were first cleaned with 1% detergent solution in an ultrasonic bath. Afterwards, they were immersed in 1 × PBS (phosphate buffer saline, pH 7.4: 137 mM NaCl, 2.7 mM KCl, 10 mM Na_2HPO_4 and 2 mM KH_2PO_4) solution with an *Escherichia coli*-expressing YadA (an adhesin from *Yersinia enterocolitica*) with an OD_{600nm} of 0.8 for 4 h [17–19]. After incubation, the PET samples were removed and washed gently with 1 × PBS buffer to remove unattached bacteria. A fluorescence microscope (Olympus BX51 from Olympus Lifescience, Tokyo, Japan), at 60× magnification, coupled with a DP71 digital camera, was used to visualise the adhered bacteria with the fluorescence imaging at a 470–490 nm excitation and a 520 nm filter in the microscope optical path. The number of bacteria in each sample was counted using ImageJ® 1.53j Software, and the reduction in bacterial adhesion was further calculated.

3. Results and Discussion

3.1. Pre-Treatment of the PET Substrate

A plasma medium consists of electrons, ions, radicals and other charged species which can be utilised for surface modifications. Polar groups such as amines, carboxylic acids, alcohols, aldehydes and esters can form on the polymer surfaces upon plasma treatment, which will eventually affect the wettability of the surfaces [2,10], and they can be used for further modification. In this study, the plasma operation parameters—power and speed—were found to significantly affect the surface properties modification process, and thus, they required optimisation. Therefore, the effects of these parameters on the PET surface properties were evaluated using the design of experiments methodology. A 2^2 full factorial design was utilised, and the water contact angle (WCA), surface energy (SFE), average roughness (R_a) and chemical composition for the PET-treated samples were measured as response variables (Table 2, Figures 1 and 2).

Table 2. Water contact angles, surface energy, average roughness and chemistry values found for the PET plasma-treated samples.

Sample	Speed (m/min)	Power (kW)	Water Contact Angle (°)	Surface Energy (mJ/m^2)			Average Surface Roughness (nm)	Surface Chemistry	
			Initial WCA	SFE Dispersed	SFE Polar	SFE Total	R_a	O/C Ratio	O Increase (%)
1	4	7.5	32 ± 1	49 ± 1	23 ± 1	72.5 ± 1	5 ± 2	0.45	40.62
2	4	15	19 ± 4	49 ± 1	28 ± 1	77 ± 1	3.95 ± 0.03	0.46	43.75
3	12	7.5	37 ± 10	49 ± 1	21 ± 5	70 ± 5	4 ± 1	0.37	15.62
4	12	15	25 ± 4	49 ± 1	26 ± 2	75 ± 2	4 ± 1	0.41	28.12
5	8	11.25	28 ± 4	49 ± 1	25 ± 2	74 ± 2	5 ± 2	0.37	15.62
6	8	11.25	28 ± 3	50 ± 1	29 ± 3	79 ± 4	4 ± 3	0.36	12.5
7	8	11.25	30 ± 5	49 ± 0.5	24 ± 2	73 ± 2	7 ± 1	0.4	25
Untreated PET	0	0	70 ± 6	42 ± 3	7 ± 3	49 ± 4	3 ± 1	0.32	0

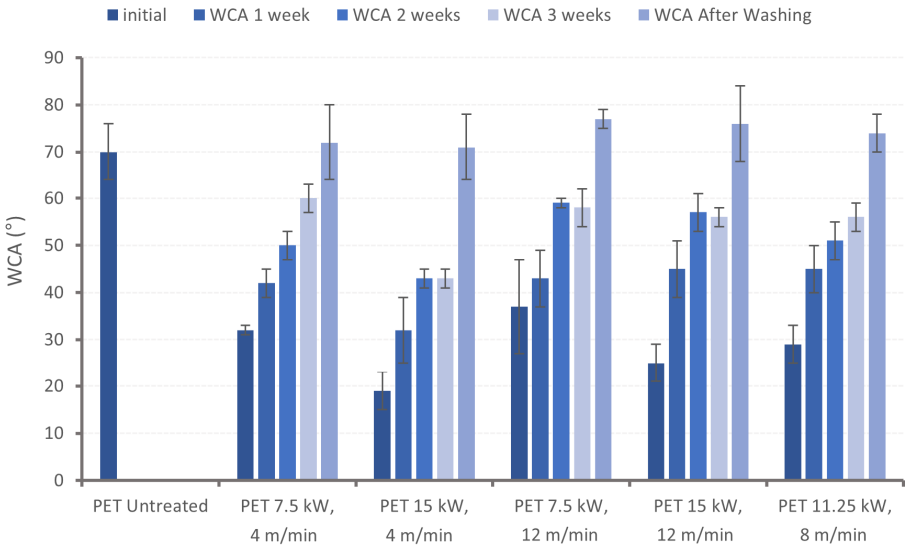

Figure 1. Water contact angle values for the PET samples after plasma treatment.

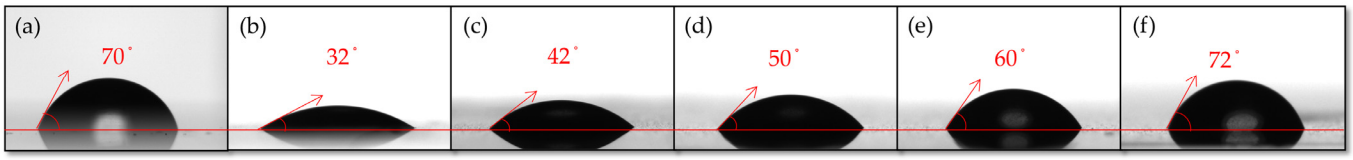

Figure 2. Representative images of the variations in the water contact angles for the PET samples: (**a**) untreated and (**b**) treated with 7.5 kW at 4 m/min. Samples (**c**–**f**) show the WCA variations for sample (**b**) after (**c**) 1 week ageing, (**d**) 2 weeks ageing, (**e**) 3 weeks ageing and (**f**) after washing.

From Figures 1 and 2, at an initial stage, it was observed that the PET surface hydrophilicity created by the plasma treatment was not permanent as it showed a recovered WCA after storing the samples at room temperature for up to 3 weeks and after washing. With only five cycles of washing, the WCA reached the initial value of the untreated PET (70 ± 6°). Additionally, the hydrophilicity loss due to ageing was lower for the sample treated at 15 kW of power with the lowest speed (4 m/min), presenting a WCA value of approximately 43 ± 2° after 3 weeks of storage. It is known that plasma-treated samples recover their hydrophobic state over time. This recovery is explained by the rotation and reorientation of the polymer chains and polar groups on the surface to reduce the interfacial surface energy [20]. The ageing and washing tests clearly showed the samples' hydrophobic state recovery. The recovery to the initial contact angle was significantly faster in water, which was consistent with the results previously reported in the literature [21].

Furthermore, Table 2 shows that the plasma treatment also changed the surface energy properties, and as expected, an overall increase in total surface energy was observed, from 49 ± 4 mJ/m^2 on untreated PET to values of between 70 and 79 mJ/m^2 on plasma-treated samples. The contribution of the polar component of the surface energy was the main element responsible for this increase, changing from 7 ± 3 mJ/m^2 on the PET control sample to values of between 21 and 29 mJ/m^2 for the PET-treated samples.

Table 3 summarises the ANOVA statistical analysis for the initial WCAs after the treatment, highlighting the significance of both of the process parameters, power and speed, for this response. A Fischer's test was used to evaluate the model significance. A model F-value of 116.04 implied that the model was significant at more than 99.95% (in this case, the *p*-value was found to be 0.0003, i.e., there was only a 0.03% chance that an F-value this large could occur due to noise).

Table 3. Analysis of variance (ANOVA) for the linear model obtained for the initial WCAs.

Source	Sum of Squares	Degree of Freedom	Mean Square	F-Value	*p*–Value	Statistical Significance
Model	186.5	2	93.25	116.04	0.0003	Significant
A-speed	30.25	1	30.25	37.64	0.0036	–
B-power	156.25	1	156.25	194.44	0.0002	–
Residual	3.21	4	0.8036	–	–	–
Lack of fit	0.5476	2	0.2738	0.2054	0.8296	Not significant
Pure error	2.67	2	1.33	–	–	–
Cor total	189.71	6	–	–	–	–

The analysis also indicated that the main factors, speed (A) and power (B), were significant, as the greatest impacts on the model were provided by power, with a confidence level of 99.98%, and speed, with a confidence level of 99.64%.

The curvature and residual lack of fit were found to be insignificant, and the proportion of variance explained by the model, which was given by the multiple coefficients of determination, R^2, was found to be 0.9831, highlighting the model's adequacy for predicting the WCAs in the design space. The obtained final model equation (Equation (1)) for the initial WCA after the treatment, in terms of actual factors, was:

$$Initial\ WCA\ (^\circ) = 41.67857 + 0.6875 \times Speed\ (\text{m min}^{-1}) - 1.66667 \times Power\ (\text{kW}) \quad (1)$$

To improve the plasma pre-treatment process, the graphical optimisation tool from Design-Expert® version 12 was used, with the intent of minimising the responses found for the WCAs (fostering a more hydrophilic surface) and maximising the amount of oxygen in comparison to the untreated sample. The upper limits (corresponding to the minimum WCA) were set as 25° for the initial WCA after the treatment and 48° for the WCA after 2 weeks of ageing, and the lower limits (minimum percentage of oxygen increase) were set at 30%.

Figure 3 shows overlay plots of power (B) versus speed (A) simultaneously for the responses fulfilling these criteria (the yellow area). Observing the yellow shaded area, it was possible to conclude that combining a plasma power above 12 kW and a treatment speed lower than 6 m/min would enable achieving the desired conditions. As such, the study was continued, setting the plasma pre-treatment conditions at the highest power (15 kW) and lowest speed (4 m/min) before beginning the UV grafting process.

To reveal the chemical composition of the samples, X-ray photoemission was used. In Table 4, detailed information about the carbon and oxygen bonds is listed. The peaks at 285.00, 286.58, 288.99 and 291.53 eV correspond to bonds typical of a benzene ring (C–C and C=C), a methylene carbon singly bound to oxygen (–C–O–) and ester carbon atoms (O–C=O), respectively. The peaks at 531.93 and 533.53 eV indicated the carbonyl oxygen (O=C) and singly bonded oxygen atoms in the ester groups (O–C). The chemical changes in the treated samples indicated by the XPS analysis mainly showed a decrease in C=C/C–C

and an increase in –C–O–bonds, which was consistent with the expected replacement of the hydrogen of the aromatic rings by the hydroxyl groups [22].

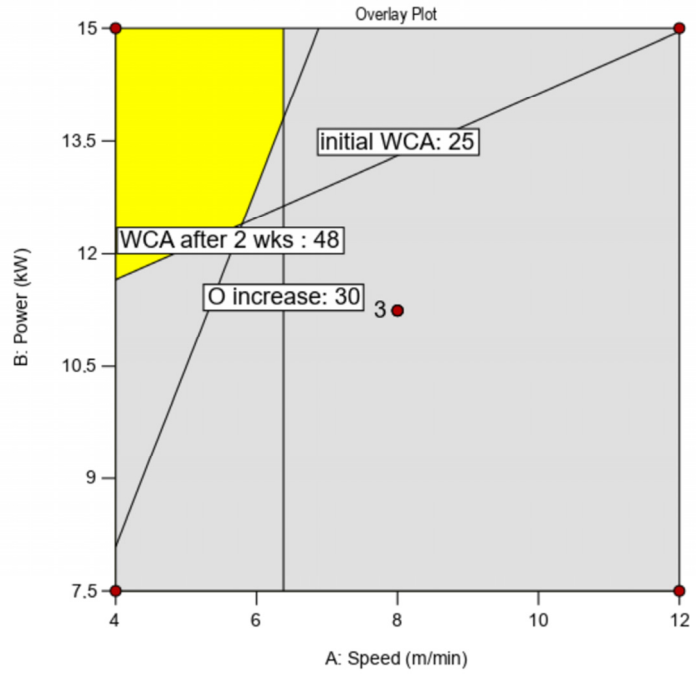

Figure 3. Overlay plots of power (B) versus speed (A).

Table 4. Relative composition (in percentages) of the different chemical groups detected with the deconvolution of the C 1s and O 1s spectra for the plasma-treated samples.

	C 1s				O 1s		O/C Ratio
Peak Deconvolution	**C1**	**C2**	**C3**	**C4**	**O1**	**O2**	**–**
Functional groups	C-C and C=C	-C-O-	O-C=O	-C=C	O=C	O-C	–
Binding energy (eV)	285.00	286.58	288.99	291.53	531.93	533.53	–
Untreated PET	44.96	15.18	13.12	2.28	11.08	13.03	0.32
Plasma-treated PET with 7.5 kW power and 4 m/min speed	37.33	14.25	14.16	3.17	12.74	17.99	0.45
Plasma-treated PET with 7.5 kW power and 12 m/min speed	39.48	15.94	14.18	2.34	10.69	16.12	0.37
Plasma-treated PET with 15 kW power and 4 m/min speed	35.29	15.94	14.3	2.27	15.99	15.52	0.46
Plasma-treated PET with 15 kW power and 12 m/min speed	38	16.56	14.06	1.95	12.43	16.49	0.41
Plasma-treated PET with 11.25 kW power and 8 m/min speed	43.46	15.09	12.78	1.59	12.93	14.3	0.38

The chemical compositions of the PET samples revealed an increase in the O 1s/C 1s ratio from 0.32 to approximately 0.40 after the plasma treatment (Table 4), with the highest ratio of 0.46 found for the PET sample treated at 15 kW power with a speed of 4 m/min. The changes in chemical composition with the introduction of these new chemical groups resulted in an increase in the hydrophilicity of the polymer surface, as indicated by the results of the WCA measurement, which showed a decrease in WCA from 70 ± 6° for the PET control to WCAs of less than 30° for the PET-plasma treated samples.

The plasma treatment could also be used to etch away surface molecules and modify the surface topography by increasing the average roughness, R_a, when enough energy

was applied [10]. In this way, the adhesion of a coating can be improved by increasing the contact points between the coating and the polymer surface [6]. The plasma-treated and the untreated PET samples were further subjected to AFM analysis to verify whether morphological changes had occurred in the PET surface topography (Figure 4). As can be seen from Figure 4, the untreated PET surface was slightly smoother (R_a = 3 nm) compared to the plasma-treated samples (R_a values ranging from 4 to 7 nm).

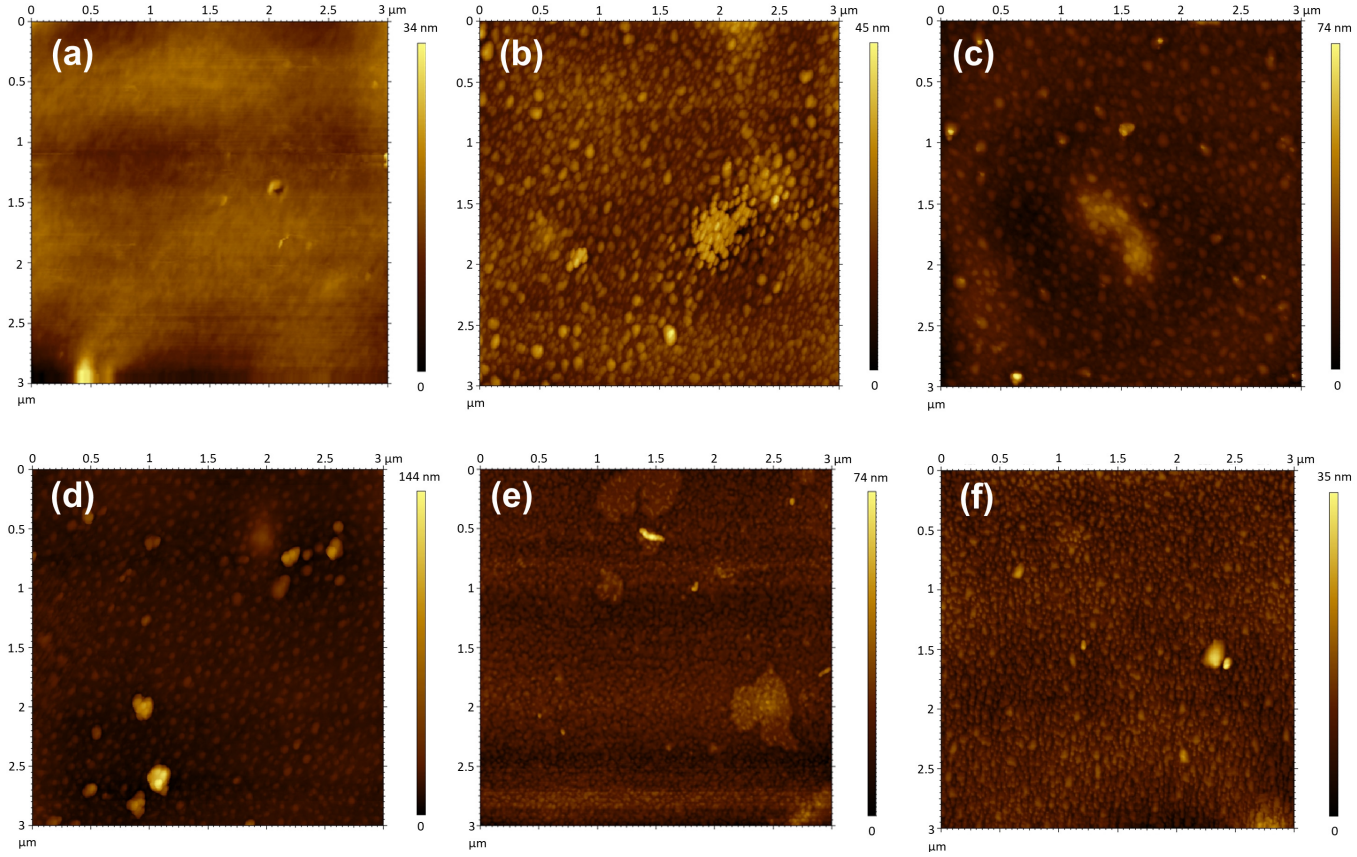

Figure 4. Surface topography images from AFM: (**a**) the untreated PET sample, and the plasma-treated samples with (**b**) 7.5 kW power and 4 m/min speed, (**c**) 15 kW power and 4 m/min speed, (**d**) 7.5 kW power 12 m/min speed, (**e**) 15 kW power and 12 m/min speed and (**f**) 11.25 kW power and 8 m/min speed.

3.2. Grafting of PET with Acrylates

Although the plasma treatment was effective for generating local hydrophilicity on the PET, the treatment was not permanent and there was a recovery of the surface hydrophobicity over time. To obtain a hydrophilic surface with a higher stability, the surfaces could be further modified with acrylates through the formation of active species, such as peroxides and hydroperoxides, to initiate the grafting process [10]. The proposed functionalisation mechanism with a plasma treatment and grafting by UV photopolymerisation can be seen in Figure 5. Even though it was not possible to identify the peroxide functional groups generated in this study, several authors have reported a similar trend with increased plasma power and time [10,23]. Thus, the lowest speed (4 m/min) and highest power (15 kW) were used to treat the samples with plasma prior to the grafting of the sodium acrylate (NaAc) and 3-sulfopropyl acrylate potassium salt (KAc). To incrementalise the plasma effect, the plasma treatment was repeated three times before beginning the UV polymerisation.

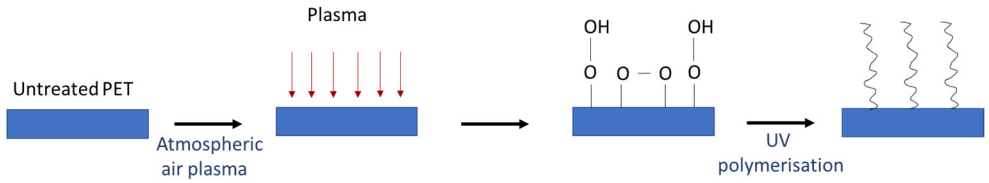

Figure 5. Proposed mechanisms for the atmospheric plasma treatment and the UV grafting polymerisation of the acrylates on the PET surface.

The plasma-treated samples were further modified with acrylates under UV light, which resulted in significant WCA reductions to 8 ± 3° (modification with NaAc), making it highly hydrophilic, and to 28 ± 13° (modification with KAc) (Table 5). The ageing tests showed that the WCAs increased to 14 ± 4°, 17 ± 9° and 16 ± 8° after 1, 2 and 3 weeks of storage for the NaAc-grafted samples, respectively, and the WCAs remained at 28–30° for the Kac-grafted samples. The washing tests for the NaAc-grafted samples suggested that the UV grafting procedure provided stability and durability to the surface treatment. However, the hydrophilicity of the Kac-treated samples after 10 washing cycles showed strong variations in the WCA results, as can be seen in Table 5, indicating that this acrylate might have led to a lower treatment uniformity. Additionally, the total surface energy of the samples increased from 49 ± 4 mJ/m^2 to 75 ± 1 mJ/m^2 for the NaAc-grafted samples and to 66 ± 7 mJ/m^2 for the Kac-grafted samples due to high increases in the polar components of the surface energy (to 38 ± 2 mJ/m^2 and 33 ± 7 mJ/m^2 for the NaAc- and Kac-modified surfaces, respectively).

Table 5. WCA, surface energy and average roughness values of the untreated, NaAc-treated and Kac-treated PET surfaces.

Samples	Initial WCA (°)	WCA after 5 Washing Cycles (°)	WCA after 10 Washing Cycles (°)	WCA after 1 Week (°)	WCA after 2 Weeks (°)	WCA after 3 Weeks (°)	SFE Dispersed (mJ/m^2)	SFE Polar (mJ/m^2)	SFE Total (mJ/m^2)	R_a (nm)
Untreated PET	70 ± 6	N/A	N/A	N/A	N/A	N/A	42 ± 3	7 ± 3	49 ± 4	2.7 ± 0.9
NaAc-grafted PET	8 ± 3	8 ± 3	14 ± 9	14 ± 4	17 ± 9	16 ± 8	37 ± 3	38 ± 2	75 ± 1	3 ± 1
Kac-grafted PET	28 ± 13	33 ± 10	55 ± 27	30 ± 11	30 ± 8	28 ± 10	33 ± 3	33 ± 7	66 ± 7	2.4 ± 0.3
No-plasma NaAc-grafted PET	39 ± 25	54 ± 12	58 ± 10	–	–	–	–	–	–	–
No-plasma Kac-grafted PET	23 ± 18	58 ± 16	77 ± 7	–	–	–	–	–	–	–

In order to confirm the effects of the plasma pre-treatment on the acrylate-grafting enhancement, the same UV grafting process was performed without any prior plasma pre-treatment, and the samples were labelled no-plasma NaAc-grafted PET and no-plasma KAc-grafted PET (Table 5). Under these conditions, the values found for the WCAs were significantly higher, indicating the positive effect of the plasma pre-treatment on the surface modification of the PET in preparation for the UV polymerisation procedure with the acrylates.

Figure 6 shows that the surface topography, as visualised by the AFM analysis, of the three-time plasma pre-treated surfaces had rougher surfaces, with R_a values of 10 ± 2 nm, and the structures resembled nanoparticle-modified surfaces. Moreover, the surface topographies of the NaAc- and Kac-treated surfaces showed smoother structures, with average roughness values (R_a) of 2.62 nm for NaAc and 2.35 nm for KAc, similar to the untreated PET sample. The difference in surface nanostructure also corroborated the successful surface modification via photopolymerisation. The unfocused surface appearance of the NaAc- and Kac-treated surfaces indicated that the AFM tip was not effective at displacing the polymer brushes and that the polymer brushes concealed the surface topography [24].

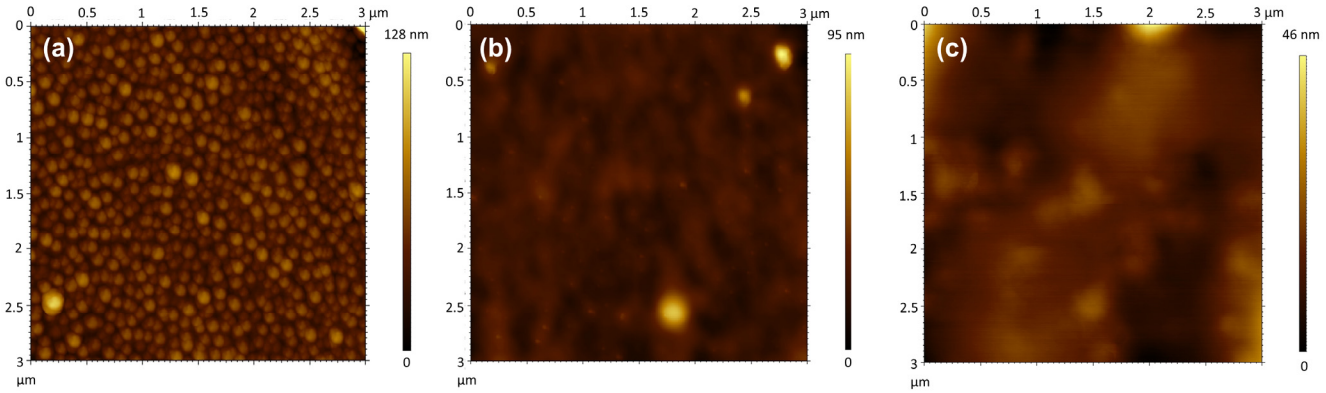

Figure 6. Surface topography images obtained by AFM for the (**a**) plasma-treated PET, with 15 kW power and 4 m/min speed; (**b**) NaAc-grafted PET; and (**c**) Kac-grafted PET.

In addition to the structural study, the thicknesses of the polymeric brushes were measured by a UV spectrophotometer using the Swanepool method, and they were found to be 28 ± 2 µm for both the NaAc- and Kac-grafted PET surfaces. This value was thicker than the conventional grafting thickness reported in the literature, and it can expand the uses of this type of polymer brush [25,26].

3.3. PET Anti-Adhesiveness

Finally, bacterial anti-adhesion studies were performed using *E. coli* expressing YadA, which is an adhesin from *Yersinia entrocolitica* [19]. Bacterial adhesins such as YadA are known to promote bacterial adhesion and biofilm formation and provide resistance to bactericidal compounds [19,27,28]. Adhesins mature the bonding between bacteria and the substrate, leading to irreversible adhesion [27]. Thus, it is important to study bacteria with such highly bonding adhesins. The bacterial adhesion onto the untreated PET and the NaAc- and KAc-treated PET samples can be seen in Figure 7. It was evident that the NaAc- and Kac-treated surfaces successfully prevented bacterial adhesion compared to the untreated PET surface. In order to quantify the effect of these modifications on the bacterial adhesion, the data gathered in Figure 7 were further analysed using ImageJ® software. The total number of cells attached to the surfaces per area (Figure 8) were counted and used to calculate the reductions in bacterial adhesion. The bacterial adhesion was reduced by 90.8% in the NaAc-grafted PET and by more than 99.9% in the KAc-grafted PET surfaces. The anti-adhesive behaviours of these types of surfaces are thought to be due to their higher hydrophilicity and surface energy [7,17]. In this way, a hydration layer is formed on the top of the surface, making it difficult for bacteria to approach [29]. According to a recent review, this reduction can be considered highly effective compared to other modifications on PET substrates [2].

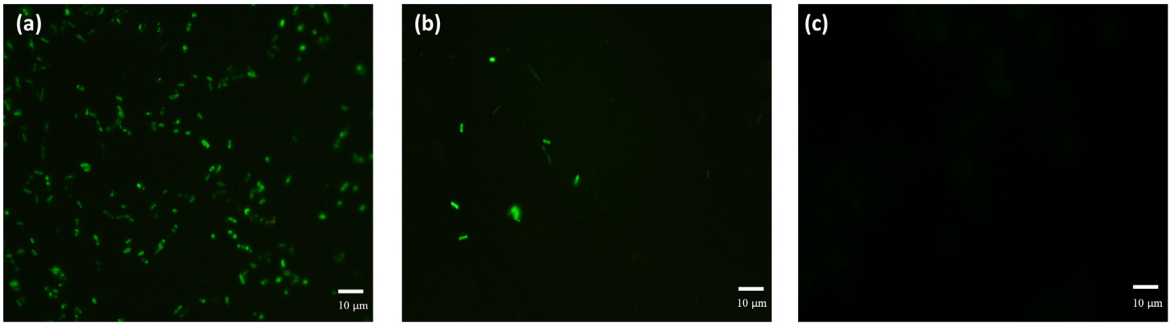

Figure 7. Fluorescence microscopy images of the *Escherichia coli* BL21 cells harboring pRSFduet_GFP and pASK_IBA2_YadA plasmids: (**a**) the untreated PET sample, (**b**) the NaAc-treated PET sample and (**c**) the KAc-treated PET sample.

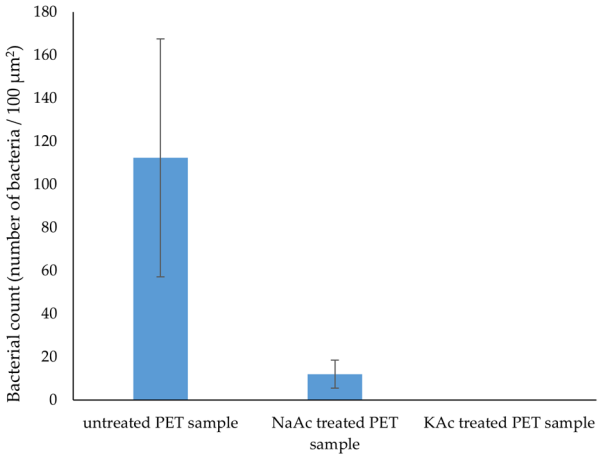

Figure 8. Number of bacteria (determined by the flourescence microscopy analysis) that attached to the untreated and treated PET surfaces after incubation for 4 h. The data are presented as means ± SDs (n = 6).

4. Conclusions

Plasma and UV treatments are cost-effective, sustainable and environmentally friendly processes, and a combination of the two can successfully avoid the use of the photoinitiator needed for UV polymerisation while increasing efficiency. Furthermore, to the best of our knowledge, the combination of UV photopolymerisation (with KAc and NaAc acrylates) with atmospheric plasma has not been studied for PET substrates.

A preliminary statistical analysis of the plasma treatment parameters showed that power and speed were significant variables influencing the surface WCAs, and the highest power and a lower speed should be used to increase the plasma effect on the PET surface. Using these conditions, plasma pre-treated PET surfaces were successfully modified with NaAc and KAc, creating hydrophilic surfaces with WCAs of lower than 10° for the NaAc-grafted samples. The studies on sample washing and ageing showed that the NaAc-treated samples remained durable under the tested conditions while the KAc-treated samples exhibited some surface heterogeneity.

Finally, the bacterial anti-adhesive performances of treated surfaces were evaluated with *E. coli*-expressing YadA, and both modified surfaces were able to inhibit bacterial adhesion by more than 90%. The combination of these two technologies can bring several benefits to the modification of conventionally hydrophobic substrates beyond being easily industrialised. Furthermore, achieving surfaces with grafting thicknesses at the level of micrometres can have other potential uses, such as implants and reservoirs to release therapeutic agents, due to higher membrane selectivity and reduced friction.

Author Contributions: Conceptualization, T.C. and C.J.S.; Methodology, T.C. and A.B.; Formal analysis, T.C.; Investigation, T.C.; Resources, L.R.R. and C.J.S.; Writing—original draft, T.C.; Writing—review & editing, T.C., S.F., A.B., J.R., L.R.R. and C.J.S.; Supervision, L.R.R. and C.J.S. All authors have read and agreed to the published version of the manuscript.

Funding: This work was supported by the ViBrANT project, which received funding from the EU Horizon 2020 Research and Innovation Programme under Marie Sklowdowska-Curie (grant agreement no. 765042), and the Portuguese Foundation for Science and Technology (FCT) (grant number UIDB/04469/2020).

Institutional Review Board Statement: Not applicable.

Informed Consent Statement: Not applicable.

Data Availability Statement: The data presented in this study are available on request from the corresponding author. The data are not publicly available due to institutional internal regulations.

Conflicts of Interest: The authors declare no conflict of interest. The funders had no role in the design of the study; in the collection, analyses or interpretation of data; in the writing of the manuscript; or in the decision to publish the results.

References

1. Suetens, C.; Latour, K.; Kärki, T.; Ricchizzi, E.; Kinross, P.; Moro, M.L.; Jans, B.; Hopkins, S.; Hansen, S.; Lyytikäinen, O.; et al. Prevalence of healthcare-associated infections, estimated incidence and composite antimicrobial resistance index in acute care hospitals and long-term care facilities: Results from two european point prevalence surveys, 2016 to 2017. *Eurosurveillance* **2018**, *23*, 1800516. [CrossRef] [PubMed]
2. Çaykara, T.; Sande, M.G.; Azoia, N.; Rodrigues, L.R.; Silva, C.J. Exploring the potential of polyethylene terephthalate in the design of antibacterial surfaces. *Med. Microbiol. Immunol.* **2020**, *209*, 363–372. [CrossRef] [PubMed]
3. Damodaran, V.B.; Murthy, N.S. Bio-inspired strategies for designing antifouling biomaterials. *Biomater. Res.* **2016**, *20*, 18. [CrossRef] [PubMed]
4. Domonkos, M.; Tichá, P.; Trejbal, J.; Demo, P. Applications of Cold Atmospheric Pressure Plasma Technology in Medicine, Agriculture and Food Industry. *Appl. Sci.* **2021**, *11*, 4809. [CrossRef]
5. Junkar, I.; Modic, M.; Mozeti, M. Modification of PET surface properties using extremely non-equilibrium oxygen plasma. *Open Chem.* **2015**, *13*, 490–496. [CrossRef]
6. Rezaei, F.; Dickey, M.D.; Bourham, M.; Hauser, P.J. Surface modification of PET film via a large area atmospheric pressure plasma: An optical analysis of the plasma and surface characterization of the polymer film. *Surf. Coat. Technol.* **2017**, *309*, 371–381. [CrossRef]
7. Katsikogianni, M.; Amanatides, E.; Mataras, D.; Missirlis, Y.F. Staphylococcus epidermidis adhesion to He, He/O2 plasma treated PET films and aged materials: Contributions of surface free energy and shear rate. *Coll. Surf. B Biointerfaces* **2008**, *65*, 257–268. [CrossRef]
8. Vazirinasab, E.; Jafari, R.; Momen, G. Evaluation of atmospheric-pressure plasma parameters to achieve superhydrophobic and self-cleaning HTV silicone rubber surfaces via a single-step, eco-friendly approach. *Surf. Coat. Technol.* **2019**, *375*, 100–111. [CrossRef]
9. Scherzer, T. VUV-Induced Photopolymerization of Acrylates. *Macromol. Chem. Phys.* **2012**, *213*, 324–334. [CrossRef]
10. Bitar, R.; Cools, P.; De Geyter, N.; Morent, R. Acrylic acid plasma polymerization for biomedical use. *Appl. Surf. Sci.* **2018**, *448*, 168–185. [CrossRef]
11. Nikiforov, A.; Ma, C.; Choukourov, A.; Palumbo, F. Plasma Technology in Antimicrobial Surface Engineering. *J. Appl. Phys.* **2022**, *131*, 011102. [CrossRef]
12. Arens, L.; Barther, D.; Landsgesell, J.; Holm, C.; Wilhelm, M. Poly(sodium acrylate) hydrogels: Synthesis of various network architectures, local molecular dynamics, salt partitioning, desalination and simulation. *Soft Matter* **2019**, *15*, 9949–9964. [CrossRef] [PubMed]
13. Bhattacharyya, R.; Chowdhury, P. Hydrogels of Acryloyl guar gum-*g*-(acrylic acid-*co*-3sulfopropylacrylate) for high-performance adsorption and release of gentamicin sulphate. *J. Polym. Res.* **2021**, *28*, 286. [CrossRef]
14. Ghasri, M.; Bouhendi, H.; Kabiri, K.; Zohuriaan-Mehr, M.J.; Karami, Z.; Omidian, H. Superabsorbent polymers achieved by surface cross linking of poly (sodium acrylate) using microwave method. *Iran. Polym. J.* **2019**, *28*, 539–548. [CrossRef]
15. Kalin, M.; Polajnar, M. The wetting of steel, DLC coatings, ceramics and polymers with oils and water: The importance and correlations of surface energy, surface tension, contact angle and spreading. *Appl. Surf. Sci.* **2014**, *293*, 97–108. [CrossRef]
16. Swanepoel, R. Determination of the thickness and optical constants of amorphous silicon. *J. Phys. E Sci. Instrum.* **1983**, *16*, 1214. [CrossRef]
17. Caykara, T.; Silva, J.; Fernandes, S.; Braga, A.; Rodrigues, J.; Rodrigues, L.R.; Silva, C. Modification of PET surfaces with gum Arabic towards its bacterial anti- adhesiveness using an experimental factorial design approach. *Mater. Today Commun.* **2021**, *28*, 102684. [CrossRef]
18. Rodrigues, J.L.; Sousa, M.; Prather, K.L.J.; Kluskens, L.D.; Rodrigues, L.R. Selection of Escherichia coli heat shock promoters toward their application as stress probes. *J. Biotechnol.* **2014**, *188*, 61–71. [CrossRef]
19. Wollmann, P.; Zeth, K.; Lupas, A.N.; Linke, D. Purification of the YadA membrane anchor for secondary structure analysis and crystallization. *Int. J. Biol. Macromol.* **2006**, *39*, 3–9. [CrossRef]
20. Morent, R.; De Geyter, N.; Leys, C.; Gengembre, L.; Payen, E. Study of the ageing behaviour of polymer films treated with a dielectric barrier discharge in air, helium and argon at medium pressure. *Surf. Coat. Technol.* **2007**, *201*, 7847–7854. [CrossRef]
21. Vesel, A.; Mozetic, M. Surface modi fi cation and ageing of PMMA polymer by oxygen plasma treatment. *Vaccum* **2012**, *86*, 634–637. [CrossRef]
22. Contini, C.; Katsikogianni, M.G.; O'Neill, F.T.; O'Sullivan, M.; Boland, F.; Dowling, D.P.; Monahan, F.J. Storage Stability of an Antioxidant Active Packaging Coated with Citrus Extract Following a Plasma Jet Pretreatment Storage Stability of an Antioxidant Active Packaging Coated with Citrus Extract Following a Plasma Jet Pretreatment. *Food Bioprocess Technol.* **2014**, *7*, 2228–2240. [CrossRef]
23. Wang, C.; Chen, J. Studies on surface graft polymerization of acrylic acid onto PTFE film by remote argon plasma initiation. *Appl. Surf. Sci.* **2007**, *253*, 4599–4606. [CrossRef]

24. Backmann, N.; Kappeler, N.; Braun, T.; Huber, F.; Lang, H.P.; Gerber, C.; Lim, R.Y.H. Sensing surface PEGylation with microcantilevers. *Beilstein J. Nanotechnol.* **2010**, *1*, 3–13. [CrossRef] [PubMed]
25. Ma, S.; Zhang, X.; Yu, B.; Zhou, F. Brushing up functional materials. *NPG Asia Mater.* **2019**, *11*, 24. [CrossRef]
26. Zeng, Y.; Xie, L.; Chi, F.; Liu, D.; Wu, H.; Pan, N.; Sun, G. Controlled Growth of Ultra-Thick Polymer Brushes via Surface-Initiated Atom Transfer Radical Polymerization with Active Polymers as Initiators. *Macromol. Rapid Commun.* **2019**, *40*, 1900078. [CrossRef] [PubMed]
27. Berne, C.; Ducret, A.; Hardy, G.G.; Brun, Y.V. Adhesins Involved in Attachment to Abiotic Surfaces by Gram-Negative Bacteria. *Microbiol. Spectr.* **2015**, *3*, MB-0018-2015. [CrossRef]
28. Schmid, Y.; Grassl, G.A.; Bühler, O.T.; Skurnik, M.; Autenrieth, I.B.; Bohn, E. Yersinia enterocolitica adhesin A induces production of interleukin-8 in epithelial cells. *Infect. Immun.* **2004**, *72*, 6780–6789. [CrossRef]
29. Maan, A.M.C.; Hofman, A.H.; De Vos, W.M.; Kamperman, M. Recent Developments and Practical Feasibility of Polymer-Based Antifouling Coatings. *Adv. Funct. Mater.* **2020**, *30*, 2000936. [CrossRef]